

Mechanism of the Reactions of Synthetic Fe–S-Based Clusters with PhCOCl: Parallel Pathways Involving Free and Coordinated Thiolate as Nucleophiles

Katie Bates, Lee Johnson, and Richard A. Henderson*

Chemistry, School of Natural Sciences, University of Newcastle, Newcastle upon Tyne, NE1 7RU, U.K.

Received July 10, 2006

Terminal thiolate ligands on the synthetic Fe–S-based clusters $[\text{Fe}_4\text{S}_4(\text{SR})_4]^{2-}$ ($\text{R} = \text{Et}$ or SPh) or $[\{\text{MoFe}_3\text{S}_4(\text{SPh})_3\}_2(\mu\text{-SPh})_3]^{3-}$ are replaced by chloride in a reaction with PhCOCl to produce $[\text{Fe}_4\text{S}_4\text{Cl}_4]^{2-}$ and $[\{\text{MoFe}_3\text{S}_4\text{Cl}_3\}_2(\mu\text{-SPh})_3]^{3-}$, respectively. Kinetic studies using stopped-flow spectrophotometry show that, in general, the mechanisms of these reactions in MeCN occur by two pathways. One pathway is independent of the concentration of PhCOCl and involves rate-limiting dissociation of the thiolate ligand. The free thiolate subsequently reacts with PhCOCl to produce PhCOSR and the Cl^- which binds to the vacant site on the cluster. The second pathway exhibits a nonlinear dependence on the concentration of PhCOCl and involves initial, rapid binding of PhCOCl to the cluster followed by intramolecular thiolate ligand attack on the coordinated acid chloride. The intermediate in which PhCOCl is bound to the cluster has been detected spectrophotometrically. The ways in which the rates of the reactions between PhCOCl and Fe–S-based clusters are affected by changes of the terminal thiolate, the metal composition of the cluster core, and the protonation state of the cluster have been investigated and are compared with the effect these same changes have on the rates of nucleophilic substitution.

Introduction

In general, mechanistic studies on the reactions of metal clusters^{1–5} are important since they establish how the reactivity of clusters differs from that of mononuclear metal complexes and particularly how the metal composition of the cluster core modulates the reactivity of the entire cluster. More specifically, mechanistic studies on synthetic Fe–S-based clusters help define the intrinsic reactivity of this particular class of cluster, which helps in understanding how natural Fe–S-based clusters may operate in certain metallo-enzymes.^{6–10}

Mechanistic chemistry of synthetic Fe–S-based clusters has, to date, included studies on the following types of reactions: nucleophilic substitution, acid-catalyzed substitution, proton transfer, binding and transformation of molecules and ions, cluster assembly and cluster disruption processes, and alkylation and electron transfer.^{2–5} However, one type of reaction which is well recognized in mononuclear complexes but which remains essentially unexplored in Fe–S-based clusters is that in which the terminal ligands behave as nucleophiles.^{11,12} In this paper, we describe, for the first time, the kinetics and mechanism of reactions of Fe–S-based

* To whom correspondence should be addressed. E-mail: r.a.henderson@ncl.ac.uk. Fax: 0191 222 6929. Tel: 0191 222 6636.

- (1) Lee, S. C.; Holm, R. H. *Chem. Rev.* **2004**, *104*, 1135.
- (2) Henderson, R. A. *Chem. Rev.* **2005**, *105*, 2365.
- (3) Henderson, R. A. *Coord. Chem. Rev.* **2005**, *249*, 1841.
- (4) (a) Daley, C. J. A.; Holm, R. H. *Inorg. Chem.* **2001**, *40*, 2785. (b) Reynolds, J. G.; Coyle, C. L.; Holm, R. H. *J. Am. Chem. Soc.* **1980**, *102*, 4350.
- (5) Wilker, J. J.; Lippard, S. J. *Inorg. Chem.* **1999**, *38*, 3569.
- (6) Holm, R. H.; Kennepohl, P.; Solomon, E. I. *Chem. Rev.* **1996**, *96*, 2239.
- (7) (a) Evans, D. J.; Henderson, R. A.; Smith, B. E. *Bioinorganic Catalysis*; Bouwmann, E., Ed.; Marcel Dekker: New York, 1999, Chapter 7. (b) Lowe, D. J.; Burgess, B. *Chem. Rev.* **1996**, *96*, 2983.

- (8) Henderson, R. A. *Nitrogen Fixation at the Millennium*; Leigh, G. J., Ed.; Elsevier: Amsterdam, 2002; Chapter 9.
- (9) Evans, D. J.; Pickett, C. *Chem. Soc. Rev.* **2003**, *32*, 268.
- (10) (a) Ragsdale, S. W.; Kumar, M. *Chem. Rev.* **1996**, *96*, 2515. (b) Grahame, D. A. *Trends Biochem. Sci.* **2003**, *28*, 221. (c) Drennan, C. L.; Peters, J. W. *Curr. Opin. Struct. Biol.* **2003**, *13*, 220. (d) Dubbek, H.; Svetlitchnyi, V.; Liss, J.; Meyer, O. *J. Am. Chem. Soc.* **2004**, *126*, 5382.
- (11) Hay, R. W. *Comprehensive Coordination Chemistry*; Wilkinson, G., Gillard, R. D., McCleverty, J. A., Eds.; Pergamon Press: New York, 1987, Vol. 6, Chapter 61.4.
- (12) Black, D. St. C. *Comprehensive Coordination Chemistry*; Wilkinson, G., Gillard, R. D., McCleverty, J. A., Eds.; Pergamon Press: New York, 1987, Vol. 6, Chapter 61.1.4.1.

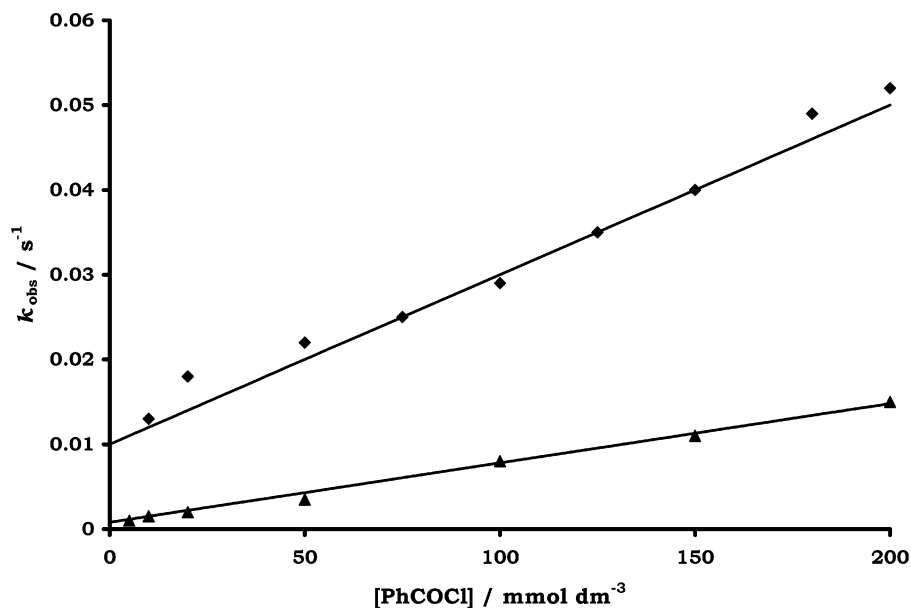
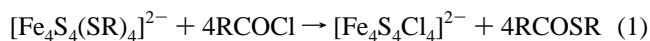


Figure 1. Dependence of k_{obs} on the concentration of PhCOCl for the reaction between PhCOCl and $[\text{Fe}_4\text{S}_4(\text{SPh})_4]^{2-}$ (◆) or $[\{\text{MoFe}_3\text{S}_4(\text{SPh})_3\}_2(\mu\text{-SPh})_3]^{3-}$ (▲) in MeCN at 25.0 °C. The lines are those defined by eq 2 and the parameters presented in the text.

clusters with acid chlorides which involve nucleophilic attack of thiolate ligands.

Earlier work^{1,13,14} has shown that the reaction of synthetic Fe–S-based clusters with acid chlorides, usually in MeCN as solvent, is a general, high-yield, and convenient method for replacing terminal thiolate ligands with chloride. One such reaction is shown in eq 1. It has been proposed that the mechanism of these reactions involves nucleophilic attack of the thiolate ligand on the acid chloride.¹³ However, there has been no mechanistic study on the reactions between synthetic Fe–S-based clusters and acid chlorides to substantiate this proposal, and the potential nucleophilicity of ligands on Fe–S-based clusters remains unproven. Herein, we report kinetic studies on the reactions between PhCOCl and $[\text{Fe}_4\text{S}_4(\text{SR})_4]^{2-}$ (R = Ph or Et) and $[\{\text{MoFe}_3\text{S}_4(\text{SPh})_3\}_2(\mu\text{-SPh})_3]^{3-}$ and show that the kinetics indicate a mechanism which is more complicated than has been proposed earlier. The mechanism of the reaction occurs by two pathways: one involving nucleophilic attack of *free* thiolate on *free* PhCOCl and the other involving nucleophilic attack of *coordinated* thiolate on *coordinated* PhCOCl. In addition to describing the kinetics and mechanism of the reaction between synthetic Fe–S-based clusters and PhCOCl, we also outline the effects that changing the thiolate ligand, the metal composition of the cluster core, and the protonation state of the cluster have on the rates of the reactions with PhCOCl. Furthermore, we compare the characteristics of the reactions with acid chlorides to the behavior observed in the substitution and acid-catalyzed substitution reactions of the same clusters² with nucleophiles.



Results and Discussion

In this paper, we report the kinetics of the reactions of PhCOCl with the cuboidal $[\text{Fe}_4\text{S}_4(\text{SR})_4]^{2-}$ (R = Ph or Et)

and $[\{\text{MoFe}_3\text{S}_4(\text{SPh})_3\}_2(\mu\text{-SPh})_3]^{3-}$. The products of these reactions are $[\text{Fe}_4\text{S}_4\text{Cl}_4]^{2-}$ and $[\{\text{MoFe}_3\text{S}_4\text{Cl}_3\}_2(\mu\text{-SPh})_3]^{3-}$, respectively. These chloro-substituted clusters have previously been isolated as the tetraalkylammonium salts and characterized by X-ray crystallography and ¹H NMR spectroscopy.^{13,14}

Kinetics of the Reactions with PhCOCl. The kinetics of the reactions between $[\text{Fe}_4\text{S}_4(\text{SR})_4]^{2-}$ (R = Et or Ph) or $[\{\text{MoFe}_3\text{S}_4(\text{SPh})_3\}_2(\mu\text{-SPh})_3]^{3-}$ and an excess of PhCOCl in MeCN were investigated using stopped-flow spectrophotometry, monitoring the change in the absorbance of the cluster. For the reactions of $[\text{Fe}_4\text{S}_4(\text{SPh})_4]^{2-}$ and $[\{\text{MoFe}_3\text{S}_4(\text{SPh})_3\}_2(\mu\text{-SPh})_3]^{3-}$, the absorbance–time traces were good fits to a single-exponential curve, indicating a first-order dependence on the concentration of cluster (Supporting Information, Figure S1). This conclusion was confirmed by studies in which $[\text{PhCOCl}] = 100 \text{ mmol dm}^{-3}$ but the concentration of cluster was varied. Over the range $[\text{Fe}_4\text{S}_4(\text{SPh})_4]^{2-} = 0.02\text{--}0.10 \text{ mmol dm}^{-3}$, the observed rate constant does not change ($k_{\text{obs}} = 0.029 \pm 0.005 \text{ s}^{-1}$).

The total change observed in the absorbance–time curves for the reactions of $[\text{Fe}_4\text{S}_4(\text{SPh})_4]^{2-}$ or $[\{\text{MoFe}_3\text{S}_4(\text{SPh})_3\}_2(\mu\text{-SPh})_3]^{3-}$ with PhCOCl correspond to the replacement of four and six thiolates, respectively. That the curves can be fitted to single exponentials indicates that replacement of the first thiolate is the slowest step in this multistep replacement reaction.

The variation of k_{obs} with the concentration of PhCOCl depends on the Fe–S-based cluster. The simplest behavior is that observed in the reactions with $[\text{Fe}_4\text{S}_4(\text{SPh})_4]^{2-}$ or $[\{\text{MoFe}_3\text{S}_4(\text{SPh})_3\}_2(\mu\text{-SPh})_3]^{3-}$ shown in Figure 1. The plots in Figure 1 show a linear dependence of k_{obs} on the

(13) Wong, G. B.; Bobrick, M. A.; Holm, R. H. *Inorg. Chem.* **1978**, *17*, 578.

(14) Palermo, R. E.; Power, P. P.; Holm, R. H. *Inorg. Chem.* **1982**, *21*, 173.

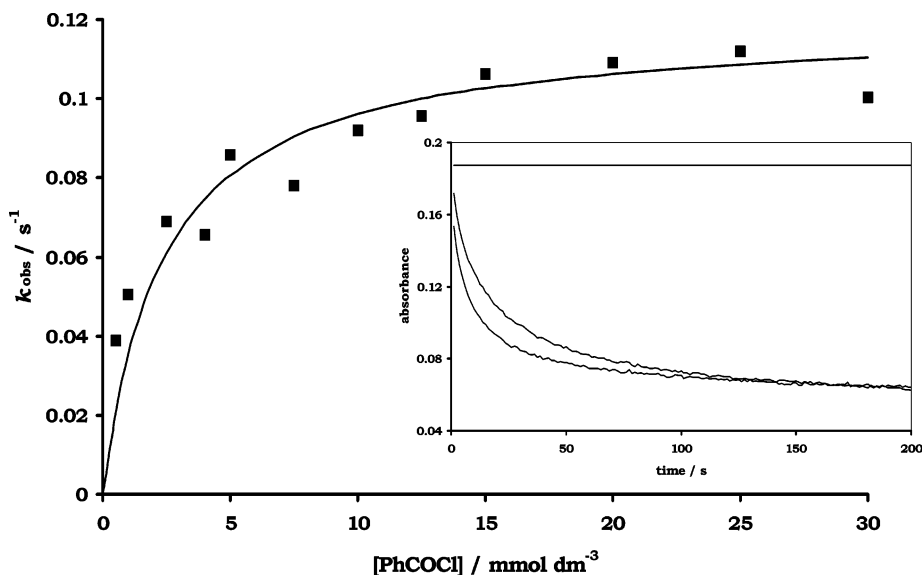


Figure 2. Dependence of k_{obs} on the concentration of PhCOCl for the reaction between PhCOCl and $[\text{Fe}_4\text{S}_4(\text{SET})_4]^{2-}$ in MeCN at 25.0°C. The curve drawn is that defined by eq 3. Insert: Stopped-flow absorbance–time curves for the reaction between $[\text{Fe}_4\text{S}_4(\text{SET})_4]^{2-}$ (0.1 mmol dm^{-3}) and PhCOCl (4.0 mmol dm^{-3}), and PhCOCl (12.5 mmol dm^{-3}) recorded at $\lambda = 455$ nm. The line with absorbance = 0.19 is the absorbance of a 0.1 mmol dm^{-3} solution of $[\text{Fe}_4\text{S}_4(\text{SET})_4]^{2-}$.

concentration of PhCOCl. However, the graphs do not go through the origin but have a finite intercept. This behavior indicates that, for both clusters the reaction occurs by two pathways, one pathway is independent of the concentration of PhCOCl (intercept) and the other exhibits a first-order dependence on the concentration of PhCOCl (gradient of the line). For both clusters, the experimental rate law has the form shown in eq 2. For $[\text{Fe}_4\text{S}_4(\text{SPh})_4]^{2-}$, $a = (1.0 \pm 0.2) \times 10^{-2} \text{ s}^{-1}$, $b = 0.20 \pm 0.02 \text{ dm}^3 \text{ mol}^{-1} \text{ s}^{-1}$; and for $[\{\text{MoFe}_3\text{S}_4(\text{SPh})_3\}_2(\mu\text{-SPh})_3]^{3-}$, $a = (8.0 \pm 0.5) \times 10^{-4} \text{ s}^{-1}$, $b = (7.0 \pm 0.5) \times 10^{-2} \text{ dm}^3 \text{ mol}^{-1} \text{ s}^{-1}$. We will discuss the interpretation of this rate law after presenting the kinetics for the reaction of $[\text{Fe}_4\text{S}_4(\text{SET})_4]^{2-}$ with PhCOCl.

$$\frac{-d[\text{cluster}]}{dt} = \{a + b[\text{PhCOCl}]\}[\text{cluster}] \quad (2)$$

The kinetics of the reaction between $[\text{Fe}_4\text{S}_4(\text{SET})_4]^{2-}$ and PhCOCl is more complicated than those for $[\text{Fe}_4\text{S}_4(\text{SPh})_4]^{2-}$ or $[\{\text{MoFe}_3\text{S}_4(\text{SPh})_3\}_2(\mu\text{-SPh})_3]^{3-}$. The absorbance–time curves {Figure 2 (insert)} for the reaction of $[\text{Fe}_4\text{S}_4(\text{SET})_4]^{2-}$ with PhCOCl can be fitted to two exponentials. The exponential nature of the curves is consistent with a first-order dependence on the concentration of $[\text{Fe}_4\text{S}_4(\text{SET})_4]^{2-}$. Biphasic absorbance–time curves have been observed in other multistep reactions of Fe–S-based clusters. It seems likely that the biphasic behavior is because the replacement of the first and second terminal thiolates have larger absorbance changes than the subsequent steps.

The kinetics of the second phase of the reaction between $[\text{Fe}_4\text{S}_4(\text{SET})_4]^{2-}$ and PhCOCl is associated with a dependence on the concentration of PhCOCl as described by eq 2, with $a = (4.3 \pm 0.2) \times 10^{-3} \text{ s}^{-1}$ and $b = 0.12 \pm 0.01 \text{ dm}^3 \text{ mol}^{-1} \text{ s}^{-1}$ (Supporting Information, Figure S2). We tentatively propose that this second phase corresponds to the reaction of PhCOCl with $[\text{Fe}_4\text{S}_4\text{Cl}(\text{SET})_3]^{2-}$ (i.e., the replacement of

the second coordinated thiolate of $[\text{Fe}_4\text{S}_4(\text{SET})_4]^{2-}$) and that the kinetics indicate $[\text{Fe}_4\text{S}_4\text{Cl}(\text{SET})_3]^{2-}$ reacts with PhCOCl by pathways analogous to those observed in the reactions of $[\text{Fe}_4\text{S}_4(\text{SPh})_4]^{2-}$ and $[\{\text{MoFe}_3\text{S}_4(\text{SPh})_3\}_2(\mu\text{-SPh})_3]^{3-}$. The kinetics of the second phase of the reaction with $[\text{Fe}_4\text{S}_4(\text{SET})_4]^{2-}$ are consistent with the mechanism that we will present below (Figure 3).

The first phase of the reaction of PhCOCl with $[\text{Fe}_4\text{S}_4(\text{SET})_4]^{2-}$ is associated with the replacement of the first coordinated thiolate. In the reactions of PhCOCl with $[\text{Fe}_4\text{S}_4(\text{SPh})_4]^{2-}$ or $[\{\text{MoFe}_3\text{S}_4(\text{SPh})_3\}_2(\mu\text{-SPh})_3]^{3-}$ (described above), it is also the first coordinated thiolate that is being replaced. Consequently, we will focus on the kinetics of the first phase of the reaction of PhCOCl with $[\text{Fe}_4\text{S}_4(\text{SET})_4]^{2-}$ which are described below.

The kinetics of the first phase of the reaction with $[\text{Fe}_4\text{S}_4(\text{SET})_4]^{2-}$ exhibits a nonlinear dependence on the concentration of PhCOCl, as shown in Figure 2 (main). Thus, at low concentrations of PhCOCl, k_{obs} increases with the concentration of acid chloride, but at higher concentrations of PhCOCl, k_{obs} is independent of the concentration of acid chloride.

Analysis of the kinetic data in Figure 2 (main) by the normal plot¹⁶ of $1/k_{\text{obs}}$ versus $1/[\text{PhCOCl}]$ gives a straight line from which the experimental rate law shown in eq 3 can be determined. The nonlinear dependence on the concentration of PhCOCl makes it difficult to establish if the curve goes through the origin or not. We have analyzed the data assuming that there is no intercept. The justification for this assumption will be discussed later.

$$\frac{-d[\text{Fe}_4\text{S}_4(\text{SET})_4]^{2-}}{dt} = \frac{(47 \pm 5)[\text{PhCOCl}][\text{Fe}_4\text{S}_4(\text{SET})_4]^{2-}}{1 + (380 \pm 40)[\text{PhCOCl}]} \quad (3)$$

The experimental rate laws (eqs 2 and 3) are consistent with the mechanism shown in Figure 3. The theoretical rate

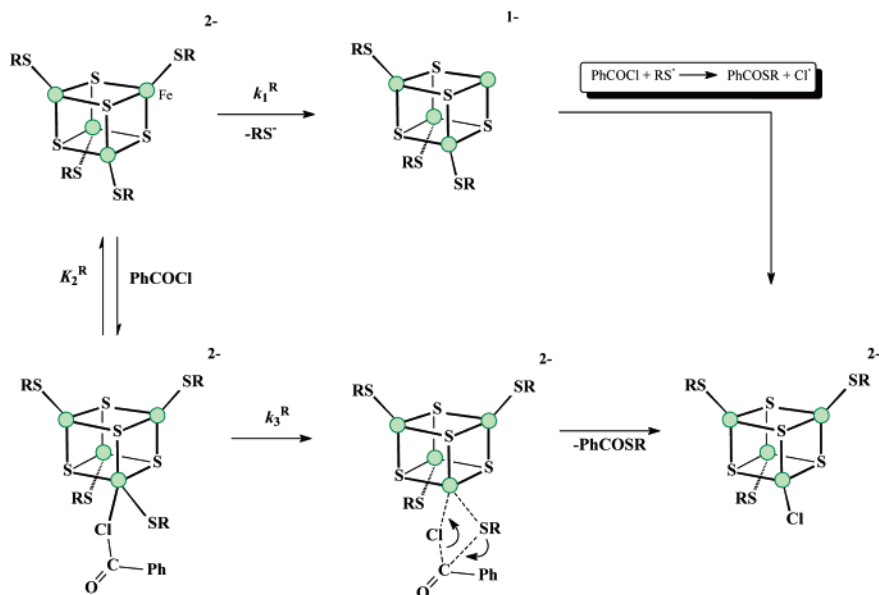


Figure 3. Mechanism for the reaction of $[\text{Fe}_4\text{S}_4(\text{SR})_4]^{2-}$ ($\text{R} = \text{Ph}$ or Et) with PhCOCl in MeCN . Analogous pathways operate for $[\{\text{MoFe}_3\text{S}_4(\text{SPh})_3\}_2(\mu\text{-SPh})_3]^{3-}$.

law associated with this mechanism is presented in eq 4. This rate law is derived assuming that binding of PhCOCl to the cluster is an equilibrium reaction which is established rapidly; prior to k_3^{R} , eq 4 is consistent with the kinetic behavior of all three Fe-S -based clusters studied herein. By comparison of eqs 3 and 4, the following values can be determined. For $[\text{Fe}_4\text{S}_4(\text{SEt})_4]^{2-}$, k_1^{Et} is undetectably small, $K_2^{\text{Et}} = 380 \pm 40 \text{ dm}^3 \text{ mol}^{-1}$ and $k_3^{\text{Et}} = 0.12 \pm 0.01 \text{ s}^{-1}$. For both $[\text{Fe}_4\text{S}_4(\text{SPh})_4]^{2-}$ and $[\{\text{MoFe}_3\text{S}_4(\text{SPh})_3\}_2(\mu\text{-SPh})_3]^{3-}$, the linear plots in Figure 1 are consistent with the mechanism shown in Figure 3 and eq 4, except with these clusters, $K_2^{\text{R}}[\text{PhCOCl}] \ll 1$ and eq 4 simplifies to eq 5. Comparison of eqs 2 and 5 gives the following values: for $[\text{Fe}_4\text{S}_4(\text{SPh})_4]^{2-}$, $k_1^{\text{Ph}} = (1.0 \pm 0.2) \times 10^{-2} \text{ s}^{-1}$, $K_2^{\text{Ph}}k_3^{\text{Ph}} = 0.20 \pm 0.02 \text{ dm}^3 \text{ mol}^{-1} \text{ s}^{-1}$, and $K_2^{\text{Ph}} \leq 0.5 \text{ dm}^3 \text{ mol}^{-1}$; for $[\{\text{MoFe}_3\text{S}_4(\text{SPh})_3\}_2(\mu\text{-SPh})_3]^{3-}$, $k_1^{\text{Mo}} = (8.0 \pm 0.5) \times 10^{-4} \text{ s}^{-1}$, $K_2^{\text{Mo}}k_3^{\text{Mo}} = (7.0 \pm 0.5) \times 10^{-2} \text{ dm}^3 \text{ mol}^{-1} \text{ s}^{-1}$ and $K_2^{\text{Mo}} \leq 0.5 \text{ dm}^3 \text{ mol}^{-1}$.

$$\frac{-d[\text{cluster}]}{dt} = \frac{\{k_1^{\text{R}} + K_2^{\text{R}}k_3^{\text{R}}[\text{PhCOCl}]\}[\text{cluster}]}{1 + K_2^{\text{R}}[\text{PhCOCl}]} \quad (4)$$

$$\frac{-d[\text{cluster}]}{dt} = \{k_1^{\text{R}} + K_2^{\text{R}}k_3^{\text{R}}[\text{PhCOCl}]\}[\text{cluster}] \quad (5)$$

In the mechanism shown in Figure 3, the PhCOCl -independent pathway (observed with $[\text{Fe}_4\text{S}_4(\text{SPh})_4]^{2-}$ and $[\{\text{MoFe}_3\text{S}_4(\text{SPh})_3\}_2(\mu\text{-SPh})_3]^{3-}$) is shown in the top line and is proposed to involve initial rate-limiting dissociation of thiolate. It seems likely that the free thiolate subsequently reacts with free PhCOCl to produce PhCOSPh and Cl^- , and the Cl^- rapidly binds to the vacant site on the cluster. Effectively, this pathway is a nucleophilic substitution reaction. Earlier studies¹⁵ have shown that the terminal thiolate ligands on $[\text{Fe}_4\text{S}_4(\text{SPh})_4]^{2-}$ undergo nucleophilic

substitution exclusively by a pathway which is independent of the concentration of nucleophile and involves rate-limiting dissociation of the thiolate $\{k_1 = (1.0 \pm 0.2) \times 10^{-2} \text{ s}^{-1}\}$. This rate constant is identical to the rate constant associated with the PhCOCl -independent pathway in the reaction with $[\text{Fe}_4\text{S}_4(\text{SPh})_4]^{2-}$ $\{k_1^{\text{Ph}} = (1.0 \pm 0.2) \times 10^{-2} \text{ s}^{-1}\}$, consistent with the proposal that thiolate dissociation is rate-limiting. The rate of nucleophilic substitution of $[\text{Fe}_4\text{S}_4(\text{SEt})_4]^{2-}$ is very slow, and the rate constant has not been measured. This is consistent with the absence of a detectable PhCOCl -independent pathway in the studies with PhCOCl .

The PhCOCl -dependent pathways for the reactions of Fe-S -based clusters is shown at the bottom of Figure 3. In this pathway, initial rapid binding of the PhCOCl to the cluster, presumably coordinating through the chloro group (K_2^{R}) or the oxygen (not shown), is followed by a sequence of steps which complete the reaction: nucleophilic attack of the coordinated thiolate on the carbonyl group of the coordinated acid chloride, dissociation of the thiolate, and transfer of the chloride to the Fe . It is not clear whether the nucleophilic attack of the coordinated thiolate precedes the chloride transfer or whether the steps are synchronous. Consequently, we cannot, at this time, unambiguously assign k_3^{R} to a particular elementary process. However, the reactivity trends which we observe (vide infra) indicate that the nucleophilic attack of the coordinated thiolate on PhCOCl is involved in the rate-limiting step.

Our interpretation of the kinetics exhibited for the reactions of PhCOCl with $[\text{Fe}_4\text{S}_4(\text{SPh})_4]^{2-}$ or $[\{\text{MoFe}_3\text{S}_4(\text{SPh})_3\}_2(\mu\text{-SPh})_3]^{3-}$ is that these represent a limiting form of eq 4 corresponding to no appreciable accumulation of the intermediate (eq 5). Consistent with this proposal, the stopped-flow absorbance–time curves for these reactions have an initial absorbance corresponding to that of the parent cluster at all concentrations of PhCOCl (Supporting Information, Figure S1). However, $[\text{Fe}_4\text{S}_4(\text{SEt})_4]^{2-}$ has a higher affinity

(15) Henderson, R. A.; Oglieve, K. E. *J. Chem. Soc., Dalton Trans.* **1993**, 1467.

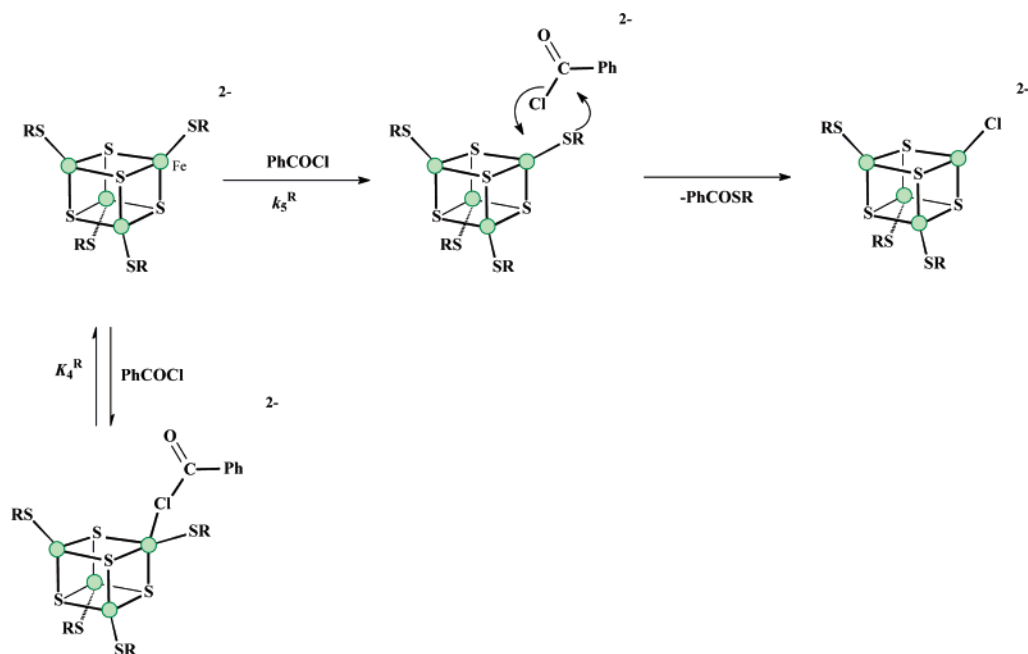


Figure 4. Mechanism for the reaction of $[\text{Fe}_4\text{S}_4(\text{SR})_4]^{2-}$ with PhCOCl in MeCN involving binding of PhCOCl to the cluster as a “dead-end” intermediate. For simplicity, the k_1^R pathway is not shown.

for binding PhCOCl than $[\text{Fe}_4\text{S}_4(\text{SPh})_4]^{2-}$, and this is consistent with some earlier observations. Studies of the binding of small molecules and ions (e.g., CO, halides, CN^- , N_3^-)^{17,16–17} showed that the binding constants with these species were larger with $[\text{Fe}_4\text{S}_4(\text{SEt})_4]^{2-}$ than $[\text{Fe}_4\text{S}_4(\text{SPh})_4]^{2-}$.

The discussion so far has focused on the interpretation of the kinetics in terms of the mechanism shown in Figure 3. However, it is important to appreciate that another mechanism (Figure 4) is also consistent with the kinetics presented above. In the mechanism shown in Figure 4, PhCOCl also binds to the cluster, but binding deactivates the acid chloride so that this is a nonproductive pathway (“dead-end” mechanism).¹⁶ The product-forming pathway is shown on the top line of Figure 4 and involves nucleophilic attack of the coordinated thiolate on *free* PhCOCl. The rate law for this “dead-end” mechanism is shown in eq 6.

$$\frac{-d[\text{cluster}]}{dt} = \frac{\{k_1^R + k_5^R[\text{PhCOCl}]\}[\text{cluster}]}{1 + K_4^R[\text{PhCOCl}]} \quad (6)$$

Equation 6 is of the same mathematical form as eq 4: the two equations differ only in the assignment of the elementary reactions associated with the terms in the numerators and denominators. Consequently, solely on the basis of the kinetics and spectroscopic changes, we cannot distinguish between the mechanisms shown in Figures 3 and 4. However, it seems unlikely that binding of PhCOCl to the cluster would result in a “dead-end” species. In contrast, binding of PhCOCl to the cluster might be expected to make the carbonyl group *more* susceptible to nucleophilic attack. On this basis, we favor the mechanism shown in Figure 3.

Table 1. Spectrophotometric Data for the Intermediate Produced within the Dead-Time of the Stopped-Flow Apparatus (2 ms) in the Reaction of $[\text{Fe}_4\text{S}_4(\text{SEt})_4]^{2-}$ with PhCOCl in MeCN at 25.0 °C^a

[PhCOCl], mmol dm ⁻³	A _T	1/(0.19 – A _T)	1/[PhCOCl], dm ³ mol ⁻¹
0.50	0.187	333	2000
1.00	0.181	111	1000
2.50	0.175	66.7	400
4.00	0.172	55.6	250
7.50	0.163	37.0	133
12.50	0.155	28.6	80

^a Data were measured at $\lambda = 455$ nm, where $\epsilon_C = 1900$ dm³ mol⁻¹ cm⁻¹, $\epsilon_{\text{int}} = 1550$ dm³ mol⁻¹ cm⁻¹, and $[\text{Fe}_4\text{S}_4(\text{SEt})_4]^{2-}_0 = 0.1$ mmol dm⁻³. A_T is the measured initial absorbance of the stopped-flow absorbance–time curve.

Spectrophotometric Detection of the Intermediate.

Figure 2 (main) shows that, for the reaction of $[\text{Fe}_4\text{S}_4(\text{SEt})_4]^{2-}$, at high concentrations of PhCOCl the rate becomes independent of the concentration of PhCOCl. This corresponds to $K_2^{\text{Et}}[\text{PhCOCl}] \gg 1$ in eq 4 and $k_{\text{obs}} = k_3^{\text{Et}}$. Under these conditions, the intermediate proposed in Figure 3, $[\text{Fe}_4\text{S}_4(\text{SR})_4(\text{ClCOPh})]^{2-}$, attains appreciable concentrations and should be spectroscopically detectable. The spectroscopic changes observed in the absorbance–time curves for the reaction between PhCOCl and $[\text{Fe}_4\text{S}_4(\text{SEt})_4]^{2-}$ {Figure 2 (insert)} are consistent with the formation of $[\text{Fe}_4\text{S}_4(\text{SEt})_4(\text{ClCOPh})]^{2-}$ within the dead-time (2 ms) of the stopped-flow apparatus.

In the reaction of PhCOCl with $[\text{Fe}_4\text{S}_4(\text{SEt})_4]^{2-}$, the initial absorbance of the stopped-flow absorbance–time curve depends on the concentration of the acid chloride {Figure 2 (insert) and Table 1}. Thus, at $\lambda = 455$ nm, when $[\text{Fe}_4\text{S}_4(\text{SEt})_4]^{2-} = 0.1$ mmol dm⁻³, the absorbance of $[\text{Fe}_4\text{S}_4(\text{SEt})_4]^{2-}$ is 0.19. However, increasing the concentration of PhCOCl results in a progressive decrease in the initial absorbance until, when $[\text{PhCOCl}] \geq 10$ mmol dm⁻³, the initial absorbance of the absorbance–time curve is 0.155.

(16) Wilkins, R. G. *Kinetics and Mechanisms of Reactions of Transition Metal Complexes*; VCH: Weinheim, 1991; pp 33–37.

(17) Henderson, R. A.; Oglieve, K. E. *J. Chem. Soc., Dalton Trans.* **1993**, 1473.

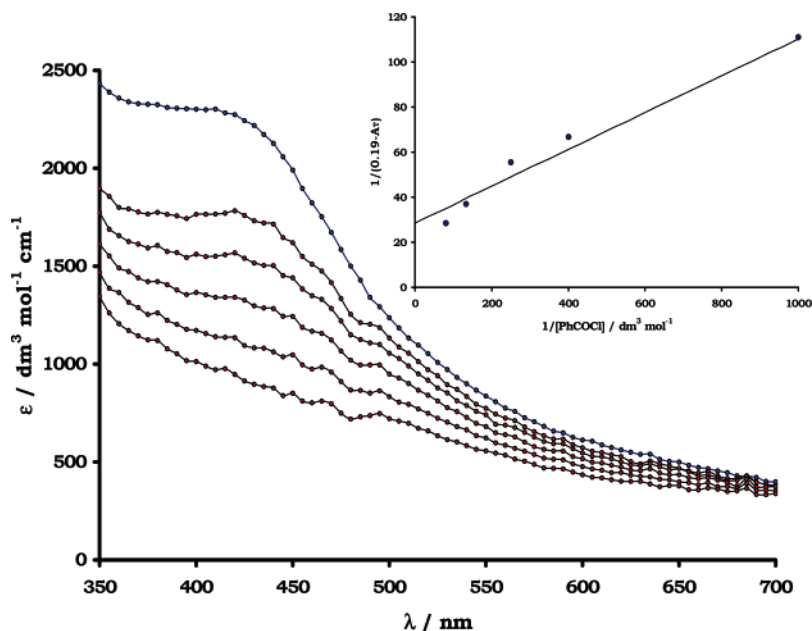


Figure 5. Visible absorption spectrum of $[\text{Fe}_4\text{S}_4(\text{SEt})_4]^{2-}$ and the time course for the reaction between $[\text{Fe}_4\text{S}_4(\text{SEt})_4]^{2-}$ (0.1 mmol dm^{-3}) and PhCOCl (20 mmol dm^{-3}) in MeCN at $25.0 \text{ }^\circ\text{C}$. Spectra were recorded at $t = 0.625, 1.25, 2.50, 5.0,$ and 10.0 s . Data points collected every 5 nm . Insert: Graphical analysis of the spectrophotometric changes observed in the reaction between PhCOCl and $[\text{Fe}_4\text{S}_4(\text{SEt})_4]^{2-}$. The data points are those presented in Table 1, and the line is that defined by eq 7 and the parameters presented in the text. A_T is the measured initial absorbance of the stopped-flow absorbance–time curve.

The variation in the initial absorbance of the stopped-flow trace is consistent with the rapid formation of an equilibrium mixture. By considering the equilibrium reaction forming $[\text{Fe}_4\text{S}_4(\text{SEt})_4(\text{CICOPh})]^{2-}$ from $[\text{Fe}_4\text{S}_4(\text{SEt})_4]^{2-}$ and PhCOCl and using Beer's Law, it can be shown that, when PhCOCl is in a large excess, the variation of the initial absorbance of the stopped-flow trace [i.e., the absorbance of the equilibrium mixture comprising $[\text{Fe}_4\text{S}_4(\text{SEt})_4]^{2-}$ and $[\text{Fe}_4\text{S}_4(\text{SEt})_4(\text{CICOPh})]^{2-}$] is related to the concentration of PhCOCl as shown in eq 7. The terms in eq 7 correspond to ϵ_C = molar extinction coefficient for $[\text{Fe}_4\text{S}_4(\text{SEt})_4]^{2-} = 1.9 \times 10^3 \text{ dm}^3 \text{ mol}^{-1} \text{ cm}^{-1}$; ϵ_{int} = molar extinction coefficient for the intermediate = $1.55 \times 10^3 \text{ dm}^3 \text{ mol}^{-1} \text{ cm}^{-1}$; A_T = initial absorbance of stopped-flow absorbance–time curve and $[\text{Fe}_4\text{S}_4(\text{SEt})_4]_0$ = concentration of $[\text{Fe}_4\text{S}_4(\text{SEt})_4]^{2-}$ added to solution = 0.1 mmol dm^{-3} .

$$\frac{1}{(\epsilon_C[\text{Fe}_4\text{S}_4(\text{SEt})_4]_0 - A_T)} = \frac{1}{(\epsilon_C - \epsilon_{\text{int}})K_2^{\text{Et}}[\text{Fe}_4\text{S}_4(\text{SEt})_4]_0[\text{PhCOCl}]} + \frac{1}{(\epsilon_C - \epsilon_{\text{int}})[\text{Fe}_4\text{S}_4(\text{SEt})_4]_0} \quad (7)$$

Inspection of eq 7 indicates that a plot of $1/(\epsilon_C[\text{Fe}_4\text{S}_4(\text{SEt})_4]_0 - A_T)$ versus $1/[\text{PhCOCl}]$ is expected to be a straight line with gradient = $1/[(\epsilon_C - \epsilon_{\text{int}})K_2^{\text{Et}}[\text{Fe}_4\text{S}_4(\text{SEt})_4]_0]$ and intercept = $1/[(\epsilon_C - \epsilon_{\text{int}})[\text{Fe}_4\text{S}_4(\text{SEt})_4]_0]$. Graphical analysis of the spectrophotometric data presented in the Table is shown in Figure 5 (insert). The linearity of this plot shows that the spectroscopically detected intermediate is formed from one PhCOCl reversibly binding to $[\text{Fe}_4\text{S}_4(\text{SEt})_4]^{2-}$. In addition, since $K_2^{\text{Et}} = \text{intercept}/\text{gradient}$ we can calculate

that $K_2^{\text{Et}} = 350 \pm 70 \text{ dm}^3 \text{ mol}^{-1}$. This value is in excellent agreement with $K_2^{\text{Et}} = 380 \pm 40 \text{ dm}^3 \text{ mol}^{-1}$ determined from the kinetics.

Using the spectral scan facility of the stopped-flow apparatus, the change in the absorption spectrum in the range $\lambda = 350\text{--}700 \text{ nm}$ during the reaction between $[\text{Fe}_4\text{S}_4(\text{SEt})_4]^{2-}$ (0.1 mmol dm^{-3}) and PhCOCl (20 mmol dm^{-3}) has been measured {Figure 5 (main)}. The top spectrum is that of $[\text{Fe}_4\text{S}_4(\text{SEt})_4]^{2-}$, while the next spectrum is that of the intermediate, $[\text{Fe}_4\text{S}_4(\text{SEt})_4(\text{CICOPh})]^{2-}$, and the remaining spectra show the subsequent formation of $[\text{Fe}_4\text{S}_4\text{Cl}_4]^{2-}$. It is evident that there is only a small difference between the spectra of $[\text{Fe}_4\text{S}_4(\text{SEt})_4]^{2-}$ and $[\text{Fe}_4\text{S}_4(\text{SEt})_4(\text{CICOPh})]^{2-}$ but the spectrum of the intermediate is less intense (particularly at lower wavelengths) than that of $[\text{Fe}_4\text{S}_4(\text{SEt})_4]^{2-}$, with a shoulder at ca. 420 nm . In common with the electronic spectra of other Fe–S-based clusters, the spectrum of $[\text{Fe}_4\text{S}_4(\text{SEt})_4(\text{CICOPh})]^{2-}$ is rather featureless.

Influence of Thiolate and Cluster Composition on the Rate of Reaction. The kinetic results presented above for the reactions of PhCOCl with $[\text{Fe}_4\text{S}_4(\text{SPh})_4]^{2-}$, $[\text{Fe}_4\text{S}_4(\text{SEt})_4]^{2-}$, or $[\{\text{MoFe}_3\text{S}_4(\text{SPh})_3\}_2(\mu\text{-SPh})_3]^{3-}$ allow us to discuss how changes to the terminal thiolate and the metal composition of the cluster affect the reactions of these clusters with acid chlorides. Furthermore, by comparison with earlier work,² we can discuss the differences in the trends in the reactivities of the three clusters with PhCOCl to that of the extensively studied nucleophilic substitution reactions of the same clusters. To facilitate the discussion, the kinetics and mechanism of nucleophilic substitution at Fe–S-based clusters will be presented in an outline.

The general mechanism for substitution of terminal ligands on Fe–S-based clusters by nucleophiles is shown in Figure

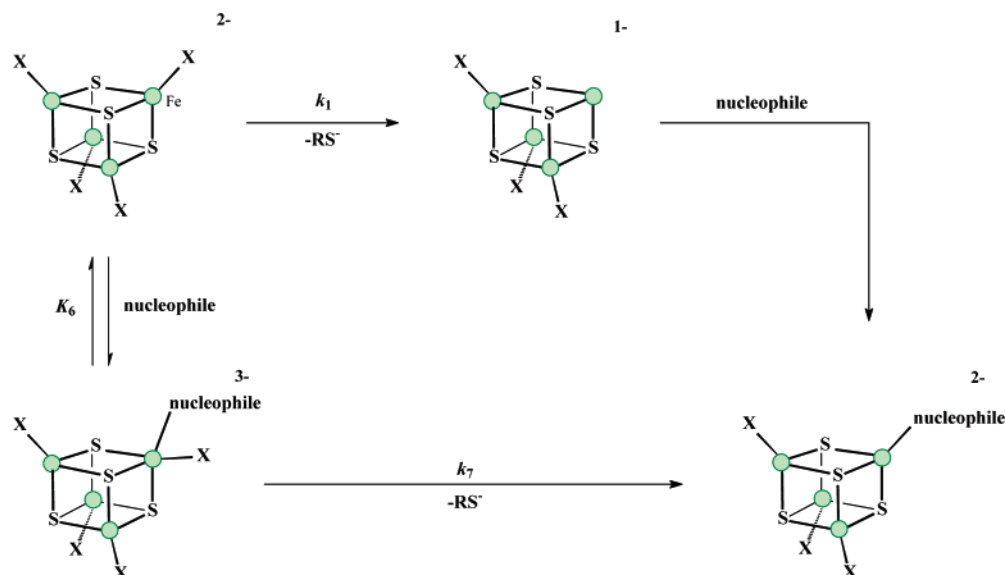


Figure 6. General mechanism for the reaction of $[\text{Fe}_4\text{S}_4\text{X}_4]^{2-}$ (X = halide or thiolate) with nucleophiles in MeCN.

6. The top pathway (k_1) occurs at a rate independent of the concentration of nucleophile and involves rate-limiting dissociation of the coordinated thiolate followed by rapid attack of the nucleophile at the vacant site on the cluster. The bottom line shows the associative pathway which comprises rapid binding of the nucleophile to the cluster (K_6) followed by rate-limiting dissociation of thiolate (k_7). The rate law for the nucleophilic substitution mechanism is shown in eq 8. It is worth noting that eq 8 is similar to the rate law for the reaction between Fe–S-based clusters and PhCOCl (eq 4).

$$\frac{-d[\text{cluster}]}{dt} = \frac{[k_1 + K_6 k_7 [\text{nucleophile}]]}{1 + K_6 [\text{nucleophile}]} [\text{cluster}] \quad (8)$$

As we have noted above, for $[\text{Fe}_4\text{S}_4(\text{SPh})_4]^{2-}$, the value of k_1 for the reaction with nucleophiles and the value of k_1^{Ph} for the reaction with PhCOCl are identical and are proposed to involve the same rate-limiting dissociation of thiolate ligand. While the PhCOCl-dependent and the nucleophile-dependent pathways have similar rate laws (eqs 4 and 8, respectively), the reactions show quite different characteristics.

Previous studies with $[\text{Fe}_4\text{S}_4(\text{SPh})_4]^{2-}$ and $[\text{Fe}_4\text{S}_4(\text{SEt})_4]^{2-}$ show that, in the nucleophilic substitution reactions, dissociation of the alkylthiolate ligand is appreciably slower than dissociation of arylthiolate ligand.² In contrast, in the reactions with PhCOCl, $[\text{Fe}_4\text{S}_4(\text{SEt})_4]^{2-}$ reacts about 250 times faster than $[\text{Fe}_4\text{S}_4(\text{SPh})_4]^{2-}$. This observation strongly indicates that lability of the coordinated thiolate is not the important factor for the PhCOCl-dependent pathway. Rather, the more electron-rich the thiolate, the faster the reaction with acid chloride, consistent with nucleophilic attack of coordinated thiolate on PhCOCl. Simplistically, the rates of the reactions of Fe–S-based clusters with acid chlorides reflect the expected nucleophilicity of the thiolate ligand

while the rates of the reactions with nucleophiles reflects the labilities of the thiolate ligands.

It is worth commenting on the relative rates of the reactions of PhCOCl with $[\text{Fe}_4\text{S}_4(\text{SPh})_4]^{2-}$ and $[\{\text{MoFe}_3\text{S}_4(\text{SPh})_3\}_2(\mu\text{-SPh})_3]^{3-}$. In both clusters, the reactions of nucleophiles or PhCOCl occur at an Fe–SPh site. Comparison of the rates of reactions of the two clusters indicates how Mo in the cluster core influences the nucleophilicity of the thiolate. It is evident from Figure 1 that $[\{\text{MoFe}_3\text{S}_4(\text{SPh})_3\}_2(\mu\text{-SPh})_3]^{3-}$ reacts with PhCOCl about 3 times slower than $[\text{Fe}_4\text{S}_4(\text{SPh})_4]^{2-}$. This observation is in accord with earlier work comparing the reactivities of $\{\text{Fe}_4\text{S}_4\}$ and $\{\text{MoFe}_3\text{S}_4\}$ clusters. For both $[\{\text{MoFe}_3\text{S}_4(\text{SPh})_3\}_2(\mu\text{-SPh})_3]^{3-}$ and $[\text{Fe}_4\text{S}_4(\text{SPh})_4]^{2-}$, comparison of the rates of acid-catalyzed nucleophilic substitution reactions¹⁷ and the binding affinities of small molecules and ions show that the Mo-containing cluster behaves as though the Fe sites were more electron-deficient. Thus, for $[\{\text{MoFe}_3\text{S}_4(\text{SPh})_3\}_2(\mu\text{-SPh})_3]^{3-}$, the associative acid-catalyzed pathway is more prevalent and the affinities for binding molecules and ions are higher than for $[\text{Fe}_4\text{S}_4(\text{SPh})_4]^{2-}$. If the Fe–SPh sites in $[\{\text{MoFe}_3\text{S}_4(\text{SPh})_3\}_2(\mu\text{-SPh})_3]^{3-}$ are more electron-deficient than those in $[\text{Fe}_4\text{S}_4(\text{SPh})_4]^{2-}$, it is reasonable that the terminal thiolate ligands on $[\{\text{MoFe}_3\text{S}_4(\text{SPh})_3\}_2(\mu\text{-SPh})_3]^{3-}$ would be less nucleophilic than those in $[\text{Fe}_4\text{S}_4(\text{SPh})_4]^{2-}$, and this would result in the slower rate of reaction with PhCOCl for the Mo-containing cluster.

Influence of Protonating the Cluster on the Rate of Reaction. One concern, when investigating the kinetics of the reaction between Fe–S-based clusters and PhCOCl, is that hydrolysis of PhCOCl by traces of adventitious water results in the formation of HCl, which would protonate the cluster. Consequently, the observed kinetics described would correspond to the reaction of PhCOCl with the protonated cluster. However, as we described above, for $[\text{Fe}_4\text{S}_4(\text{SPh})_4]^{2-}$, the agreement in the values of k_1^{Ph} from the studies with PhCOCl and k_1 for nucleophile substitution (where adventi-

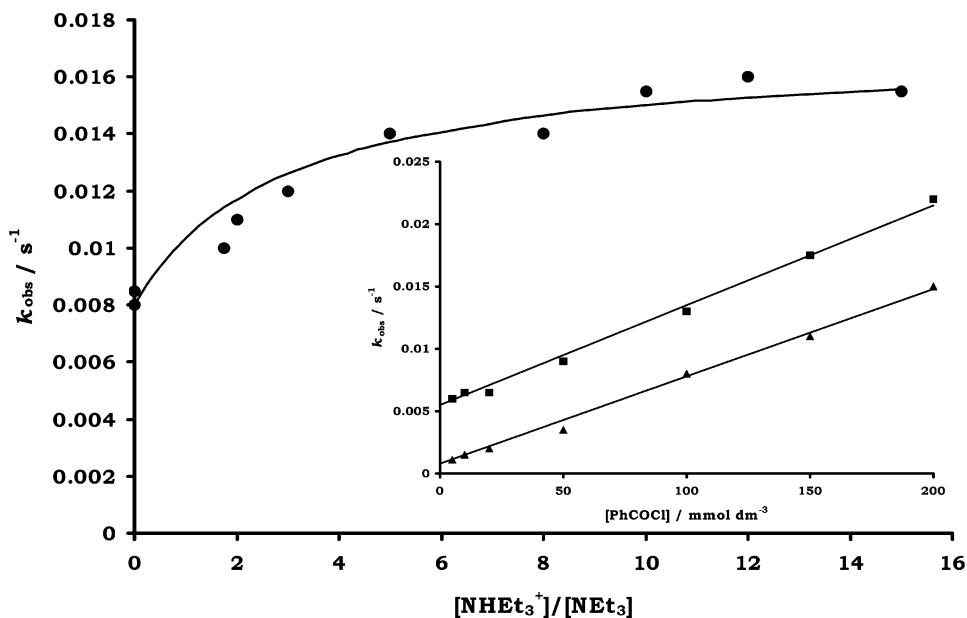


Figure 7. Kinetic data for the reaction between PhCOCl and $\{[\text{MoFe}_3\text{S}_4(\text{SPh})_3\}_2(\mu\text{-SPh})_3\}^{3-}$ in MeCN at 25.0 °C. Main: Dependence of k_{obs} on $[\text{NHEt}_3^+]/[\text{NEt}_3]$, when $[\text{PhCOCl}] = 100 \text{ mmol dm}^{-3}$. The curve drawn is that defined by eq 9 and the rate and equilibrium constants described in the text. Insert: Dependence of k_{obs} on $[\text{PhCOCl}]$ when $[\text{NHEt}_3^+]/[\text{NEt}_3] = 0$ (\blacktriangle) or $[\text{NHEt}_3^+]/[\text{NEt}_3] = 5.0$ (\blacksquare). Lines drawn are those defined by eq 9 and the rate and equilibrium constants presented in the text.

tious acid cannot be present) indicates that the kinetics described above are those of the unprotonated cluster. Furthermore, the effect of deliberately adding acid to the reaction between PhCOCl and Fe–S-based clusters, described below, substantiates this conclusion.

Previous studies^{2,3} have shown that $[\text{NHEt}_3^+]$ ($pK_{\text{a}} = 18.46$ in MeCN)¹⁸ is capable of protonating synthetic Fe–S-based clusters in MeCN. Characteristic features of the protonation of synthetic Fe–S-based clusters in the presence of mixtures of $[\text{NHEt}_3^+]$ and NEt_3 are as follows. (i) Protonation of Fe–S-based clusters increases the rate of both the associative and dissociative nucleophilic substitution pathways. (ii) The rate of substitution depends on the ratio $[\text{NHEt}_3^+]/[\text{NEt}_3]$ (not on the absolute concentrations of either acid or base). (iii) The pK_{a} 's of all synthetic Fe–S-based clusters in MeCN fall in the narrow range $pK_{\text{a}} = 17.9\text{--}18.9$, irrespective of the nuclearity, topology, overall charge, or terminal ligands of the cluster, indicating that protonation occurs at a common site on the clusters, presumed to be the bridging sulfur atoms. (iv) It seems likely that a coordinated thiolate sulfur is more basic than a bridged sulfur, and so it is expected that initial rapid protonation of a thiolate occurs prior to protonation of the bridged sulfur. The labilization of the coordinated thiolate by protonation of both the thiolate and a bridged sulfur has been discussed in some detail before.² For the benefit of the subsequent discussion, we will briefly outline the electronic origins of how protonation of the cluster labilizes the coordinated thiolates to dissociation. Protonation of a thiolate ligand to produce a thiol affects the Fe–S bonding in the following ways. The coordinated thiol has weaker S-to-Fe σ -bond, but stronger Fe-to-S π -back-bond than the corresponding coordinated thiolate. The overall effect is that

protonation of the thiolate ligand produces a coordinated thiol whose lability is not appreciably different from that of the thiolate. However, addition of a second proton to the cluster, this time at a bridged sulfur, results in a decrease of the Fe-to-S π -back-bonding to the coordinated thiol and thus increases the lability of the thiol to dissociation.

We have investigated how the protonation state of $\{[\text{MoFe}_3\text{S}_4(\text{SPh})_3\}_2(\mu\text{-SPh})_3\}^{3-}$ affects the kinetics of the reaction between this cluster and PhCOCl. The kinetics of the reaction between $\{[\text{MoFe}_3\text{S}_4(\text{SPh})_3\}_2(\mu\text{-SPh})_3\}^{2-}$ and PhCOCl have been studied in the presence of mixtures of $[\text{NHEt}_3^+]$ and NEt_3 . At a constant concentration of PhCOCl, over the range $[\text{NHEt}_3^+]/[\text{NEt}_3] = 0\text{--}15$, k_{obs} increases in a nonlinear fashion, as shown in Figure 7 (main). Thus, at low values of $[\text{NHEt}_3^+]/[\text{NEt}_3]$, the rate increases with $[\text{NHEt}_3^+]/[\text{NEt}_3]$, but at high values of the ratio, the rate is independent of $[\text{NHEt}_3^+]/[\text{NEt}_3]$. In complementary experiments, where the ratio $[\text{NHEt}_3^+]/[\text{NEt}_3] = 5.0$ is kept constant, the rate increases in a linear fashion as the concentration of PhCOCl is increased {Figure 7 (insert)}. An important point about these kinetics is that the rate depends only on the ratio $[\text{NHEt}_3^+]/[\text{NEt}_3]$, not the absolute concentrations of either the acid or base. An analogous dependence on the ratio $[\text{NHEt}_3^+]/[\text{NEt}_3]$ is observed in the nucleophilic substitution reactions of this cluster².

The rate law for the reaction between PhCOCl and $\{[\text{MoFe}_3\text{S}_4(\text{SPh})_3\}_2(\mu\text{-SPh})_3\}^{3-}$ in the presence of mixtures of $[\text{NHEt}_3^+]$ and NEt_3 is shown in eq 9, where k_1^{Mo} and $K_2^{\text{Mo}}k_3^{\text{Mo}}$ are the rate constants for the reaction of $\{[\text{MoFe}_3\text{S}_4(\text{SPh})_3\}_2(\mu\text{-SPh})_3\}^{3-}$ with PhCOCl in the absence of acid, while $k_8^{\text{Mo}} = (5.5 \pm 0.5) \times 10^{-3} \text{ s}^{-1}$ and $k_9^{\text{Mo}} = (8.0 \pm 0.5) \times 10^{-2} \text{ dm}^3 \text{ mol}^{-1} \text{ s}^{-1}$ are the values for the corresponding reactions of the protonated cluster. $K_0 = 0.35 \pm 0.05$ is the equilibrium constant for protonation of the cluster.

(18) Izutsu, K. *Acid–Base Dissociation Constants in Dipolar Aprotic Solvents*; Blackwell Scientific, Oxford, 1990.

$$-\frac{d[\text{MoFe}_3]}{dt} = \frac{\{(k_1^{\text{Mo}} + K_2^{\text{Mo}}k_3^{\text{Mo}}[\text{PhCOCl}]) + (k_8^{\text{Mo}} + k_9^{\text{Mo}}[\text{PhCOCl}]K_0[\text{NHEt}_3^+]/[\text{NEt}_3])\}[\text{MoFe}_3]}{1 + K_0[\text{NHEt}_3^+]/[\text{NEt}_3]} \quad (9)$$

Equation 9 is consistent with the mechanism shown in Figure 8. The initial steps in this mechanism are identical to those previously described in the acid-catalyzed nucleophilic substitution reactions of $[\{\text{MoFe}_3\text{S}_4(\text{SPh})_3\}_2(\mu\text{-SPh})_3]^{3-}$ and involve rapid protonation of the thiolate ligand and a bridging sulfur^{2,3,17} prior to any interaction with PhCOCl. As has been argued in the acid-catalyzed nucleophilic substitution reactions, it seems likely that the thiolate sulfur is the most basic site and initial protonation of the thiolate produces the corresponding thiol within the dead-time of the stopped-flow apparatus. Subsequent protonation of the cluster core is also rapid but produces an equilibrium mixture of clusters in which a bridged sulfur is either protonated or not. The amount of cluster with a protonated bridged sulfur depends on the ratio $[\text{NHEt}_3^+]/[\text{NEt}_3]$. Since both protonation of the thiolate and bridged sulfur occur before the interaction with PhCOCl, the value of K_0 , and hence the calculated $\text{p}K_a = 18.0$ for the protonated cluster, determined from the studies with PhCOCl are in good agreement with the values established in the studies on the acid-catalyzed nucleophilic substitution reactions² of $[\{\text{MoFe}_3\text{S}_4(\text{SPh})_3\}_2(\mu\text{-SPh})_3]^{3-}$, where protonation of the cluster precedes binding of the nucleophile ($K_0 = 0.26 \pm 0.03^{17}$ and $\text{p}K_a = 18.1$)².

Protonation of $[\{\text{MoFe}_3\text{S}_4(\text{SPh})_3\}_2(\mu\text{-SPh})_3]^{3-}$ leads to an increase in the overall rate of the reaction with PhCOCl. However, inspection of the data {Figure 7 (insert)} shows that this overall rate increase is attributable, almost exclusively, to the increase in the PhCOCl-independent pathway ($k_6^{\text{Mo}}/k_1^{\text{Mo}} = 6.9$). The PhCOCl-dependent pathway is essentially unaffected by protonation of the cluster ($k_7^{\text{Mo}}/K_2^{\text{Mo}}k_3^{\text{Mo}} = 1.1$). The effect that protonation of the cluster has on the two pathways with PhCOCl stands in stark contrast to the effect protonation has on the two nucleophilic substitution pathways. Kinetic studies on the acid-catalyzed nucleophilic substitution reactions of $[\{\text{MoFe}_3\text{S}_4(\text{SPh})_3\}_2(\mu\text{-SPh})_3]^{3-}$ shows that both the nucleophile-independent and the nucleophile-dependent pathways are facilitated by protonation of the cluster.^{2,3} Clearly, the markedly different effects that protonation of the cluster has on the rates of the substrate-dependent pathways in the reactions with PhCOCl or nucleophile further supports our conclusion that the intimate mechanism for the PhCOCl-dependent pathway is different than that of the associative pathway for nucleophilic substitution.

We would expect that, for the PhCOCl-independent pathway, protonation of the thiolate and bridged sulfur would increase the rate of the reaction since this pathway is rate-limited by the dissociation of the terminal ligand. Protonation of the cluster labilizes the cluster toward dissociation.

That protonation of $[\{\text{MoFe}_3\text{S}_4(\text{SPh})_3\}_2(\mu\text{-SPh})_3]^{3-}$ has little effect on the PhCOCl-dependent pathway is interesting. Consideration of the elementary steps involved in the PhCOCl-dependent pathway indicate that the following factors could be important: (i) binding of PhCOCl to the

protonated cluster would be more favorable than to the parent cluster; (ii) protonation of the cluster would diminish the nucleophilicity of the terminal ligand but (iii) facilitate the transfer of the chloro-group from PhCOCl to iron and dissociation of the thiol. Thus, in the reactions of the protonated and parent cluster, there are conflicting effects in the elementary steps for the PhCOCl-dependent pathway, and the overall effect is that protonation of the cluster has little effect on the rate of this pathway.

A detail of the reaction between $[\{\text{MoFe}_3\text{S}_4(\text{SPh})_3\}_2(\mu\text{-SPh})_3]^{3-}$ and PhCOCl in the presence of acid which deserves further comment concerns the identity of the nucleophile. In Figure 8, we have indicated that the nucleophile is the coordinated thiol, but of course, the PhCOCl could be attacked by one of the coordinated thiolates on the cluster. Nonetheless, protonation anywhere on the cluster would be expected to diminish the nucleophilicity even of the coordinated thiolates. Even if a coordinated thiolate is the nucleophile, the marginal effect that protonation of the cluster has on the rate of the PhCOCl-dependent pathway indicates that, for this pathway, each of the elementary steps in the transformation of the acid chloride (binding of acid chloride, nucleophilic attack, and chloride transfer) are affected differently by protonation of the cluster.

Summary

Herein we have presented, for the first time, the kinetics of the reaction between synthetic Fe–S-based clusters and PhCOCl. Specifically, we have studied the reactions of the cuboidal $[\text{Fe}_4\text{S}_4(\text{SR})_4]^{2-}$ ($\text{R} = \text{Et}$ or Ph) and $[\{\text{MoFe}_3\text{S}_4(\text{SPh})_3\}_2(\mu\text{-SPh})_3]^{3-}$. In general, the reaction occurs by two pathways. One pathway involves initial rate-limiting dissociation of thiolate from the parent cluster followed by attack of chloride (produced from the reaction of the free thiolate with acid chloride) at the vacant cluster site. The other pathway involves nucleophilic attack of a thiolate ligand on the coordinated acid chloride. Both the kinetics and spectrophotometric analysis are consistent with the acid chloride binding to the cluster with the concentration of the intermediate $[\{\text{Fe}_4\text{S}_4(\text{SEt})_4(\text{ClCOPh})\}^{2-}]$ accumulating sufficiently that it is detectable at high concentrations of PhCOCl.

The general trends in the reactions of Fe–S-based clusters with PhCOCl reflect (i) changes to the lability of the thiolate for the PhCOCl-independent pathway and (ii) changes to the nucleophilicity of the terminal thiolates for the PhCOCl-dependent pathway. Thus, alkylthiolate ligands are better nucleophiles but are less labile than arylthiolate ligands, and hence, the reaction of PhCOCl with $[\text{Fe}_4\text{S}_4(\text{SEt})_4]^{2-}$ is faster than with $[\text{Fe}_4\text{S}_4(\text{SPh})_4]^{2-}$ but occurs exclusively by the PhCOCl-dependent pathway.

For all the clusters studied in this work, the reaction with PhCOCl occurs at the Fe sites. Comparison of the reactivities of $[\{\text{MoFe}_3\text{S}_4(\text{SPh})_3\}_2(\mu\text{-SPh})_3]^{3-}$ and $[\text{Fe}_4\text{S}_4(\text{SPh})_4]^{2-}$ shows

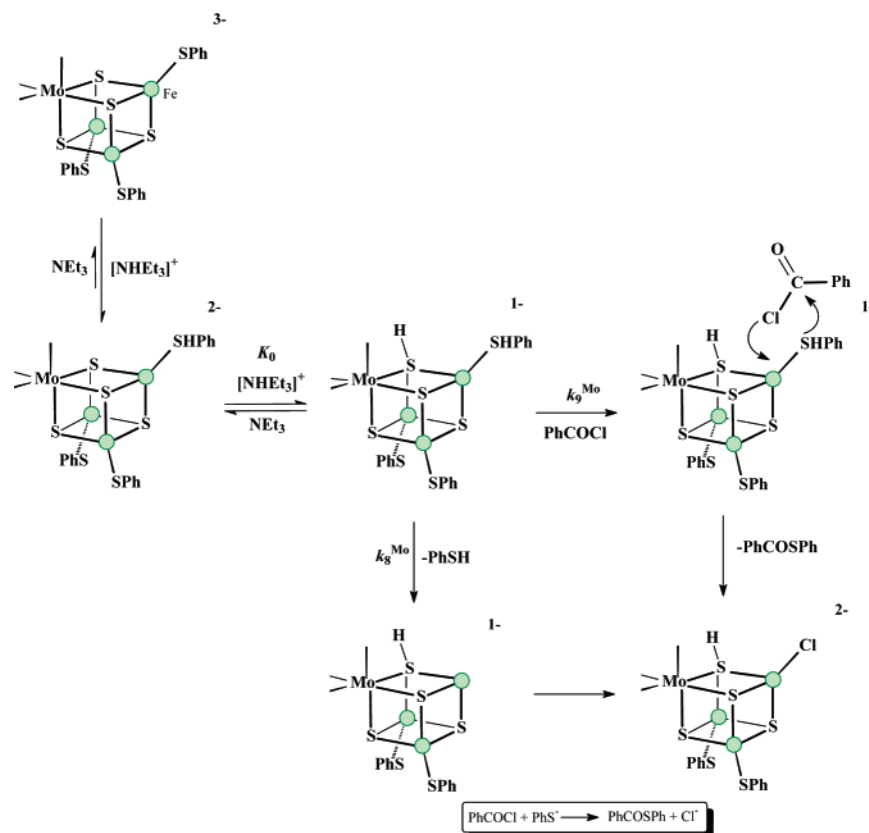


Figure 8. Mechanism for the reaction of $[\{\text{MoFe}_3\text{S}_4(\text{SPh})_3\}_2(\mu\text{-SPh})_3]^{3-}$ with PhCOCl in the presence of $[\text{NHEt}_3]^+$ in MeCN. For clarity, only one of the $\{\text{MoFe}_3\text{S}_4(\text{SPh})_3\}$ subclusters is shown.

that the Fe–SPh residues in the $\{\text{MoFe}_3\text{S}_4\}$ cluster react slower than those in the $\{\text{Fe}_3\text{S}_4\}$ cluster. This observation is in accord with earlier conclusions that Mo within a cuboidal Fe–S-based cluster has an electron-withdrawing effect on the Fe sites.

The protonation state of the cluster influences the rate of the reaction with PhCOCl . Earlier studies on the kinetics of the acid-catalyzed nucleophilic substitution reactions of synthetic Fe–S-based clusters indicate that protonation can occur at both the terminal thiolate ligands and a bridged sulfur of the cluster core. For the PhCOCl -independent pathway, protonation of the cluster facilitates the reaction with PhCOCl since protonation labilizes the cluster to dissociation. Intuitively, it might be anticipated that protonation of the cluster would diminish the nucleophilicity of the coordinated thiolate. Intriguingly, the PhCOCl -dependent pathway is little affected by the protonation state of the cluster. The intimate mechanism of the PhCOCl -dependent pathway must involve not only the nucleophilic attack of the coordinated thiolate on the coordinated acid chloride (expected to be inhibited by protonation of the cluster) but also dissociation of the Fe–thiolate bond and transfer of chloride from acid chloride to Fe (both expected to be facilitated by protonation). The overall effect on all these elementary processes is a negligible difference in the rates of reactions of the protonated and unprotonated clusters with PhCOCl .

It is instructive to compare the mechanisms we have proposed for the reactions of PhCOCl with nucleophiles

coordinated to Fe–S-based clusters and that observed for reactions of free nucleophiles with acid chlorides (acyl transfer reactions). In principle, there are three mechanisms for these reactions (Figure 9).

We are unaware of any kinetic studies on the reaction of PhS^- with PhCOCl . However, there have been some detailed studies on the hydrolysis of $\text{RC}_6\text{H}_4\text{COCl}$ which indicate that the mechanism involves the acylium ion.¹⁹ Although there is little unambiguous evidence for the existence of the acylium ion (e.g., reactions involving PhCOCl show no common ion chloride effect), there is much evidence that the mechanism involves a transition state with dissociative character (e.g., benzoyl chloride derivatives containing electron-donating R substituents hydrolyze faster). Only in benzoyl chloride derivatives where the R substituent is very electron-withdrawing (e.g., nitro-group) is an associative mechanism indicated.

Clearly, the kinetics of the reactions of PhCOCl with the Fe–S-based clusters described herein are not consistent with the involvement of the acylium ion, but rather indicate an associative mechanism. This is consistent with the observation that benzoyl chloride derivatives containing electron-withdrawing substituents favor an associative mechanism. The binding of PhCOCl to the cluster presumably withdraws electron density from the acid chloride and facilitates nucleophilic attack by the coordinated thiolate.

(19) Song, B. D.; Jencks, W. P. *J. Am. Chem. Soc.* **1989**, *111*, 8470 and references therein.

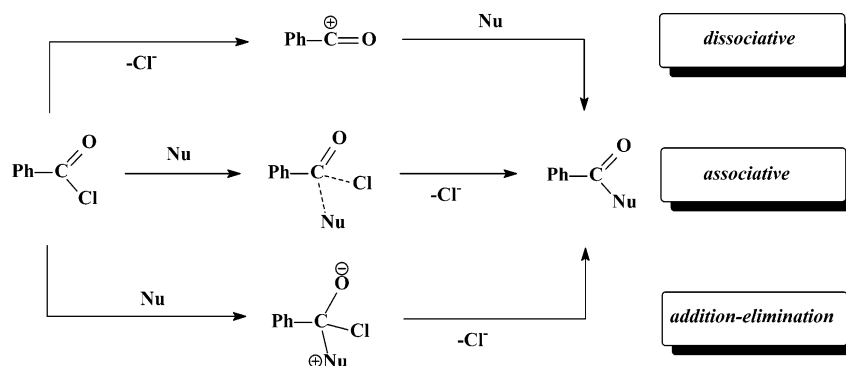


Figure 9. Possible mechanisms for the reaction of PhCOCl with nucleophiles.

Finally, the studies reported herein indicate the ability of terminal thiolate ligands on synthetic Fe–S-based clusters to be nucleophiles in reactions with coordinated acid chlorides. The question arises “What other substrates are susceptible to attack by thiolates coordinated to Fe–S-based clusters?”

It has been reported²⁵ that the reactions of $[\text{Fe}_4\text{S}_4(\text{SEt})_4]^{2-}$ with RNC (R = Buⁿ, Bu^t, or 4-ClC₆H₄NC) in the presence of an excess of EtSH produces RN=C(H)SEt. There is spectrophotometric evidence that BuⁿNC coordinates to the cluster, and a mechanism involving nucleophilic attack of coordinated thiolate on coordinated BuⁿNC has been proposed. It remains to be seen what other substrates (e.g., esters, alkenes, alkynes, etc.) undergo intramolecular nucleophilic attack from thiolates coordinated to synthetic Fe–S-based clusters.

Experimental Section

All manipulations were performed under an atmosphere of dinitrogen using Schlenk or syringe techniques as appropriate. All solvents used were dried and distilled under an atmosphere of dinitrogen immediately prior to use. The clusters $[\text{NBu}^n_4]_2[\text{Fe}_4\text{S}_4(\text{SPh})_4]$,²⁰ $[\text{NEt}_4]_2[\text{Fe}_4\text{S}_4(\text{SEt})_4]$,²¹ and $[\text{NBu}^n_4]_3[\{\text{MoFe}_3\text{S}_4(\text{SPh})_3\}_2(\mu\text{-SPh})_3]$ ²² were prepared by the methods described in the literature¹¹ and characterized by comparison with the reported ¹H NMR spectra.

Purification of Benzoyl Chloride. Benzoyl chloride (100 mL) in THF (65 mL) was washed with two portions of cold 5% NaHCO₃ in distilled water (50 mL) to give a cloudy solution. Addition of

calcium chloride gave a clear solution. The THF was removed by distillation at atmospheric pressure, and the benzoyl chloride was fractionally distilled in vacuo.

Kinetic Studies. The kinetics were studied using an Applied Photophysics SX.18MV stopped-flow spectrophotometer, modified for use with air-sensitive solutions. The temperature was maintained by recirculating water from a Grant LT D6G thermostat tank. All kinetic studies were performed under pseudo-first-order conditions²³ with all reagents at least in a 10-fold excess over the concentration of cluster. All kinetics were measured at 25 °C. Absorbance changes were monitored at $\lambda = 455$ nm. The absorbance–time traces were fitted to a single-exponential curve using the Applied Photophysics kinetics software to determine the observed rate constant (k_{obs}). The values of k_{obs} presented in Figures 1 and 3 are the average of three experiments. The dependences of k_{obs} on PhCOCl and $[\text{NHEt}_3^+]/[\text{NEt}_3]$ were determined by graphical methods, as described in the Results and Discussion.

All solutions for the kinetic studies were prepared in MeCN under a dinitrogen atmosphere and were used within 1 h. Transfer of the solutions into the stopped-flow apparatus was by means of all-glass, gastight syringes.

The solutions used in the studies involving $[\text{NHEt}_3]^+$ and NEt_3 were prepared from separate stock solutions of $[\text{NHEt}_3][\text{BPh}_4]$ and NEt_3 . $[\text{NHEt}_3][\text{BPh}_4]$ was prepared by the method described in the literature and characterized by comparison with the reported ¹H NMR spectrum.²⁴

Acknowledgment. We thank the EPSRC for a studentship (K.B.).

Supporting Information Available: Kinetic data for the reactions of $[\text{Fe}_4\text{S}_4(\text{SR})_4]^{2-}$ (R = Ph or Et) and $[\{\text{MoFe}_3\text{S}_4(\text{SPh})_3\}_2(\mu\text{-SPh})_3]^{3-}$ with PhCOCl; stopped-flow absorbance–time curves for the reaction of $[\text{Fe}_4\text{S}_4(\text{SPh})_4]^{2-}$ with PhCOCl, and a graph showing the dependence of k_{obs} on the concentration of PhCOCl for the second phase of the reaction with $[\text{Fe}_4\text{S}_4(\text{SEt})_4]^{2-}$. This material is available free of charge via the Internet at <http://pubs.acs.org>.

IC0612707

(20) Christou, G.; Garner, C. D.; Balasubramanian, A.; Ridge, B.; Rydon, H. N. *Inorg. Synth.* **1982**, *21*, 33.

(21) Averill, B. A.; Herskovitz, T.; Holm, R. H.; Ibers, J. A. *J. Am. Chem. Soc.* **1973**, *95*, 3523.

(22) Christou, G.; Garner, C. D. *J. Chem. Soc., Dalton Trans.* **1980**, 2354.

(23) Espenson, J. H. *Chemical Kinetics and Reaction Mechanisms*; McGraw-Hill: New York, 1981.

(24) Dilworth, J. R.; Henderson, R. A.; Dahlstrom, P.; Nicholson, T.; Zubieta, J. A. *J. Chem. Soc., Dalton Trans.* **1987**, 529.

(25) Schwartz, A.; E. E. van Tamelen, *J. Am. Chem. Soc.* **1977**, *99*, 3189.